Journal of Solid Mechanics Vol. 1, No. 2 (2009) pp. 108-117

Simple Solutions for Buckling of Conical Shells Composed of Functionally Graded Materials

A. Lavasani*

Department of Mechanical Engineering, Islamic Azad University, Arak Branch, Arak, Iran

Received 5 April 2009; accepted 15 June 2009

ABSTRACT

Using Donnell-type shell theory a simple and exact procedure is presented for linear buckling analysis of functionally graded conical shells under axial compressive loads and external pressure. The solution is in the form of a power series in terms of a particularly convenient coordinate system. By analyzing the buckling of a series of conical shells, under various boundary conditions and different material coefficients, the validity of the presented procedure is confirmed.

Keywords: Buckling; Conical shells; Functionally graded material; Axial load

1 INTRODUCTION

DUE to their extensive use, particularly in the aeronautical industry, the buckling of conical shells has been studied by many researchers. Much literature exists on the buckling of isotropic conical shells under compressive axial loads [1-8] and under external pressure [3, 9, 10], as well as combined loading [11]. A simple formula was developed for the buckling of isotropic conical shells by Siede and Calif [1] and later verified by Lackman and Renzien [2]. Siede's formula is independent of boundary conditions and is best for long shells. Using complex series Singer [9] and Baruch and Singer [10] proposed a procedure for solving the three equilibrium equations and two out-of-plane boundary conditions are satisfied identically while the out-of-plane equilibrium equation and in-plane boundary condition are satisfied approximately. Subsequently, Baruch et al. [7] improved Singer's solution by satisfying the in-plane boundary conditions exactly. To our knowledge there has not been a simple solution for buckling analysis of isotropic and functionally graded conical shells under axial loads and external pressure. In the following, we develop a simple and exact procedure for buckling analysis of isotropic and functionally graded conical shells under axial compression and external pressure. The procedure consists of following steps:

I. The buckling equations are developed and expressed in terms of displacements;
II. Using a new technique, exact solution are constructed in series form for the governing equations;
III. By way of verification, several examples are analyzed and the effects of boundary conditions and elastic coefficients on the buckling loads are investigated.

2 DONNELL-TYPE GOVERNING EQUATIONS

Consider a conical shell as shown in Fig.1 that R_1 and R_2 indicate the radii of the cone at its small and large ends, respectively, α denotes the semi-vertex angle of the cone and L is the cone length along its generator. We introduce the $x-\theta$ coordinate system; x is measured along the cone's generator starting at the middle length and θ is the circumferential coordinate. The displacements of the shell's middle surface are denoted by U and V along x and θ-

* *E-mail address*: ali_lavas@yahoo.com.

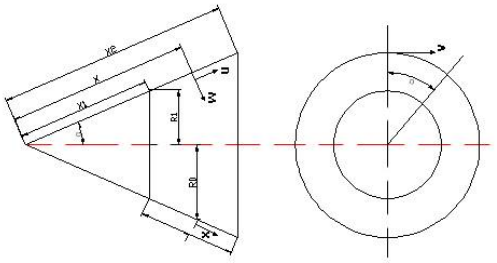

Fig. 1
Geometry and notations for a typical cone.

direction respectively, and by W along the normal to the surface (inward positive). In terms of these variables the cone's radius at any point along its length may be expressed as:

$$R(x) = R_\circ + x\sin\alpha \tag{1}$$

Now let the cone be subjected to an axially compressive load P and external normal pressure q. Under this loading the membrane stress resultant, at the critical state, may be expressed as:

$$\begin{aligned} N_{x\circ} &= \frac{P + q\pi(2R_\circ + x\sin\alpha)x\sin\alpha}{2\pi R(x)\cos\alpha} \\ N_{\theta\circ} &= \frac{qR(x)}{\cos\alpha} \end{aligned} \tag{2}$$

These equations based on the membrane theory of shallow shells degenerate to their more familiar forms for cylindrical shells when α is set equal to zero. For linear buckling analysis of composite conical shells, under P and q loadings, we adopt the shallow shell theory of Donnell-type and write the governing equations derived in [12], as:

$$\begin{aligned} &L_{11}U + L_{12}V + L_{13}W = \circ \\ &L_{21}U + L_{22}V + L_{23}W = \circ \\ &L_{31}U + L_{32}V + (L_{33} + L_N)W = \circ \end{aligned} \tag{3}$$

where

$$L_{11} = C\frac{\partial^2}{\partial x^2} + \frac{C\sin\alpha}{R(x)}\frac{\partial}{\partial x} - \frac{C\sin^2\alpha}{R^2(x)} + \frac{(1-\nu)C}{2R^2(x)}\frac{\partial^2}{\partial\theta^2}$$

$$L_{12} = \frac{(1+\nu)C}{2R(x)}\frac{\partial^2}{\partial x\partial\theta} - \frac{(3-\nu)C\sin\alpha}{2R^2(x)}\frac{\partial}{\partial\theta}$$

$$L_{21} = \frac{(1+\nu)C}{2R(x)}\frac{\partial^2}{\partial x\partial\theta} + \frac{(3-\nu)C}{2R^2(x)}\frac{\partial}{\partial\theta}$$

$$L_{22} = \frac{1-\nu}{2}C\left[\frac{\partial^2}{\partial x^2} + \frac{\sin\alpha}{R(x)}\frac{\partial}{\partial x} - \frac{\sin^2\alpha}{R^2(x)}\right] + \frac{C}{R^2(x)}\frac{\partial^2}{\partial\theta^2}$$

$$L_{13} = -\frac{\nu C\cos\alpha}{R(x)}\frac{\partial}{\partial x} + \frac{C\sin\alpha\cos\alpha}{R^2(x)}$$

$$L_{23} = L_{32} = \frac{C\cos\alpha}{R^2(x)}\frac{\partial}{\partial\theta}$$

$$L_{31} = \frac{-\nu C\cos\alpha}{R(x)}\frac{\partial}{\partial x} - \frac{C\sin\alpha\cos\alpha}{R^2(x)}$$

$$L_{33}=\frac{C\cos^2\alpha}{R^2(x)}+D\frac{\partial^4}{\partial x^4}+\frac{2D}{R^2(x)}\frac{\partial^4}{\partial x^2\partial\theta^2}+\frac{D}{R^4(x)}\frac{\partial^4}{\partial\theta^4}+\frac{2D\sin\alpha}{R(x)}\frac{\partial^3}{\partial x^3}$$
$$-\frac{2D\sin\alpha}{R^3(x)}\frac{\partial^3}{\partial x\partial\theta^2}-\frac{D\sin^2\alpha}{R^2(x)}\frac{\partial^2}{\partial x^2}+\frac{4D\sin^2\alpha}{R^4(x)}\frac{\partial^2}{\partial\theta^2}+\frac{D\sin^3\alpha}{R^3(x)}\frac{\partial}{\partial x}$$
$$L_N=\frac{1}{R(x)}\frac{\partial}{\partial x}[R(x)N_{x\circ}\frac{\partial}{\partial x}]+\frac{1}{R^2(x)}\frac{\partial}{\partial\theta}(N_{\theta\circ}\frac{\partial}{\partial\theta}) \tag{4}$$

where C and D are calculated from the following equations:

$$C=\frac{1}{1-\nu^2}\int_{-h/2}^{+h/2}E(z)\mathrm{d}z$$
$$D=\frac{1}{1-\nu^2}\int_{-h/2}^{+h/2}E(z)z^2\mathrm{d}z \tag{5}$$

where

$$E(z)=(E(c)-E(m))(\frac{z}{h}+\frac{1}{2})^k+E(m) \tag{6}$$

where $E(z)$ is material elastic constants for functionally graded material (FGM) [13], in that $E(m)$ and $E(c)$ are material elastic constants for metal and ceramic and k is a constant ratio; h is the wall thickness. The force and moment stress resultant are expressed in terms of the displacements U, V, W by:

$$\begin{Bmatrix}N_x\\N_\theta\\N_{x\theta}\\M_x\\M_\theta\\M_{x\theta}\end{Bmatrix}=\begin{bmatrix}l_{11}&l_{12}&l_{13}\\l_{21}&l_{22}&l_{23}\\l_{31}&l_{32}&l_{33}\\\circ&\circ&l_{43}\\\circ&\circ&l_{53}\\\circ&\circ&l_{63}\end{bmatrix}\begin{Bmatrix}U\\V\\W\end{Bmatrix} \tag{7}$$

where

$$l_{11}=C\frac{\partial}{\partial x}-\frac{\nu C\sin\alpha}{R(x)},\qquad l_{12}=\frac{\nu C}{R(x)}\frac{\partial}{\partial\theta},\qquad l_{13}=-\frac{\nu C\cos\alpha}{R(x)}$$
$$l_{21}=\nu C\frac{\partial}{\partial x}+\frac{C\sin\alpha}{R(x)},\qquad l_{22}=\frac{C}{R(x)}\frac{\partial}{\partial x},\qquad l_{23}=-\frac{C\cos\alpha}{R(x)}$$
$$l_{31}=\frac{(1-\nu)C}{2R(x)}\frac{\partial}{\partial\theta},\qquad l_{32}=\frac{(1-\nu)}{2}C\left(\frac{\partial}{\partial x}-\frac{\sin\alpha}{R(x)}\right)$$
$$l_{43}=-D\frac{\partial^2}{\partial x^2}-\nu D\frac{\sin\alpha}{R(x)}\frac{\partial}{\partial x}-\frac{\nu D}{R^2(x)}\frac{\partial^2}{\partial\theta^2}$$
$$l_{53}=-\nu D\frac{\partial^2}{\partial x^2}-\frac{D\sin\alpha}{R(x)}\frac{\partial}{\partial x}-\frac{D}{R^2(x)}\frac{\partial^2}{\partial\theta^2}$$
$$l_{63}=\frac{-(1-\nu)}{2R(x)}D\frac{\partial}{\partial x}\left[\frac{1}{R(x)}\frac{\partial}{\partial\theta}\right] \tag{8}$$

For simplicity, let us first consider the following two types of boundary conditions [14]:

Case 1: Simply-supported boundary condition at $x = \pm L/2$.

Case 2: Clamped boundary conditions at $x = \pm L/2$.

3 EXACT SOLUTIONS

An inspection of the differential operators $L_{i,j}(i,j = 1,2,3)$ in Eq. (4) reveals the following properties: The coefficients of all these operators are functions of x only, i.e. they are independent of θ. Now let us assume solutions for equation (12) in following form:

$$\begin{aligned} U &= u(x)\cos n\theta \\ V &= v(x)\sin n\theta \\ W &= w(x)\cos n\theta \end{aligned} \tag{9}$$

where

$$\begin{aligned} u(x) &= \sum_{m=\circ}^{\infty} a_m x^m \\ v(x) &= \sum_{m=\circ}^{\infty} b_m x^m \\ w(x) &= \sum_{m=\circ}^{\infty} c_m x^m \end{aligned} \tag{10}$$

where n is an integer representing the circumferential wave number of the buckled shell and a_m, b_m and c_m are constants to be determined later. On substituting from Eqs. (9) and (10) into Eq. (3) and using Eqs. (1) and (4), we develop three linear algebraic equations by matching the terms of same order in x. In addition we obtain the following recurrence relations:

$$\begin{aligned} a_{m+2} &= G_{1,1}a_{m+1} + G_{1,2}a_m + G_{1,3}b_{m+1} + G_{1,4}b_m + G_{1,5}C_{m+1} + G_{1,6}C_m \\ b_{m+2} &= G_{2,1}a_{m+1} + G_{2,2}a_m + G_{2,3}b_{m+1} + G_{2,4}b_m + G_{2,5}C_m \\ C_{m+4} &= G_{3,1}a_{m+1} + G_{3,2}a_m + G_{3,3}a_{m-1} + G_{3,4}a_{m-2} + G_{3,5}b_m + G_{3,6}b_{m-1} + G_{3,7}b_{m-2} + G_{3,8}C_{m+3} + G_{3,9}C_{m+2} \\ &\quad + G_{3,10}C_{m+1} + G_{3,11}C_m + G_{3,12}C_{m-1} + G_{3,13}C_{m-2} + G_{3,14}C_{m-3}, \qquad (m=0,1,2,\ldots) \end{aligned} \tag{11}$$

The above recurrence relations allow one to express the unknown constants $a_\circ$, a_1, $b_\circ$, b_1, $c_\circ$, c_1, c_2, and c_3. The coefficients $G_{i,j}$ are given by following relation:

$$G_{1,1} = -\frac{(2m+1)\sin\alpha}{(m+2)R_\circ}$$

$$G_{1,2} = -\frac{m^2\sin^2\alpha}{(m+2)(m+1)R_\circ^2} + \frac{2\sin^2\alpha + (1-\nu)n^2}{2R_\circ^2(m+2)(m+1)}$$

$$G_{1,3} = -\frac{(1+\nu)n}{2R_\circ(m+2)}$$

$$G_{1,4} = -\frac{[(1+\nu)m - (3-\nu)]n\sin\alpha}{2R_\circ^2(m+2)(m+1)}$$

$$G_{1,5}=\frac{\nu\cos\alpha}{R_\circ(m+2)}$$

$$G_{1,6}=\frac{(\nu m-1)\sin\alpha\cos\alpha}{R_\circ^2(m+2)(m+1)}$$

$$G_{2,1}=\frac{(1+\nu)n}{(1-\nu)R_\circ(m+2)}$$

$$G_{2,2}=\frac{[(1+\nu)m+(3-\nu)]n\sin\alpha}{(1-\nu)R_\circ^2(m+2)(m+1)}$$

$$G_{2,3}=G_{1,1}$$

$$G_{2,4}=-\frac{m^2\sin^2\alpha}{R_\circ^2(m+2)(m+1)}+\frac{(1-\nu)\sin^2\alpha+2n^2}{(1-\nu)R_\circ^2(m+2)(m+1)}$$

$$G_{2,5}=-\frac{2n\cos\alpha}{(1-\nu)R_\circ^2(m+2)(m+1)}$$

$$G_{3,1}=\frac{\nu C\cos\alpha}{DR_\circ(m+4)(m+3)(m+2)}$$

$$G_{3,2}=\frac{C(3\nu m+1)\sin\alpha\cos\alpha}{DR_\circ^2(m+4)(m+3)(m+2)(m+1)}$$

$$G_{3,3}=\frac{C[3\nu(m-1)+2]\sin^2\alpha\cos\alpha}{DR_\circ^3(m+4)(m+3)(m+2)(m+1)}$$

$$G_{3,4}=\frac{C[\nu(m-2)+1]\sin^3\alpha\cos\alpha}{DR_\circ^4(m+4)(m+3)(m+2)(m+1)}$$

$$G_{3,5}=\frac{Cn\cos\alpha}{DR_\circ^2(m+4)(m+3)(m+2)(m+1)}$$

$$G_{3,6}=\frac{Cn\sin 2\alpha}{DR_\circ^3(m+4)(m+3)(m+2)(m+1)}$$

$$G_{3,7}=\frac{Cn\sin^2\alpha\cos\alpha}{DR_\circ^4(m+4)(m+3)(m+2)(m+1)}$$

$$G_{3,8}=-\frac{2(2m+1)\sin\alpha}{R_\circ(m+4)}$$

$$G_{3,9}=\frac{1}{(m+4)(m+3)}[\frac{2n^2+\sin^2\alpha}{R_\circ^2}-\frac{P}{2\pi DR_\circ\cos\alpha}+\frac{6m^2\sin^2\alpha}{R_\circ^2}]$$

$$G_{3,10}=[-\frac{q(m+1)\tan\alpha}{D}-\frac{3Pm\sin\alpha}{2\pi DR_\circ^2\cos\alpha}-\frac{2m(m-1)(2m-1)\sin^3\alpha}{R_\circ^3}$$
$$+\frac{1}{(m+4)(m+3)(m+2)}\frac{(2n^2+\sin^2\alpha)(2m-1)\sin\alpha}{R_\circ^3}]$$

$$G_{3,11}=[D\sin^2\alpha(2n^2+\sin^2\alpha)m(m-2)-CR_\circ^2\cos^2\alpha-Dn^4+\frac{qn^2R_\circ^3}{\cos\alpha}$$
$$-Dm(m-1)^2(m-2)\sin^4\alpha+4Dn^2\sin^2\alpha-4qR_\circ^3m\tan\alpha\sin\alpha-\frac{3PR_\circ m(m-1)\sin^2\alpha}{2\pi\cos\alpha}$$
$$-3.5qR_\circ^3m(m-1)\tan\alpha\sin^2\alpha]/DR_\circ^4(m+4)(m+3)(m+2)(m+1)$$

$$G_{3,12}=[-(\frac{P}{2\pi\cos\alpha}+\frac{4.5qR_\circ^2}{\cos\alpha})(m-1)(m-2)\sin^3\alpha-6qR_\circ^2(m-1)\tan\alpha\sin^2\alpha$$
$$-2CR_\circ\sin\alpha\cos^2\alpha+\frac{3qR_\circ^2n^2\sin\alpha}{\cos\alpha}]/DR_\circ^4(m+4)(m+3)(m+2)(m+1)$$
$$G_{3,13}=[-0.5q\tan\alpha R_\circ(m-2)(5m-7)\sin^3\alpha+3qn^2R_\circ\tan\alpha\sin\alpha$$
$$-C\sin^2\alpha\cos^2\alpha]/DR_\circ^4(m+4)(m+3)(m+2)(m+1)$$
$$G_{3,14}=\frac{1}{DR_\circ^4(m+4)(m+3)(m+2)(m+1)}\left[\left(-0.5q(m-2)(m-3)\frac{\sin^2\alpha}{\cos\alpha}-\frac{qn^2}{\cos\alpha}\right)\sin^3\alpha\right] \quad (12)$$

Therefore the general form of $u(x), v(x)$ and $w(x)$ may be written as:

$$u(x)=u_1(x)a_\circ+u_2(x)a_1+u_3(x)b_\circ+u_4(x)b_1+u_5(x)c_\circ+u_6(x)c_1+u_7(x)c_2+u_8(x)c_3$$
$$v(x)=v_1(x)a_\circ+v_2(x)a_1+v_3(x)b_\circ+v_4(x)b_1+v_5(x)c_\circ+v_6(x)c_1+v_7(x)c_2+v_8(x)c_3 \quad (13)$$
$$w(x)=w_1(x)a_\circ+w_2(x)a_1+w_3(x)b_\circ+w_4(x)b_1+w_5(x)c_\circ+w_6(x)c_1+w_7(x)c_2+w_8(x)c_3$$

In which $u_i(x), v_i(x)$ and $w_i(x)$ $(i=1,2,...,8)$ are the base functions of $u(x)$, $v(x)$ and $w(x)$ respectively, and $a_\circ, a_1, b_\circ, b_1, c_\circ, c_1, c_2$, and c_3 are the unknowns to be determined by imposing the boundary conditions at both ends of the cone. The critical buckling loads and the corresponding buckling mode shapes can finally be obtained by equating the determinants of the coefficients matrix obtained after imposing the eight boundary conditions to zero.

4 NUMERICAL RESULTS AND DISCUSSIONS

4.1. Numerical results for isotropic conical shell

In this section numerical results are presented for the buckling of isotropic conical shells under axial compression with different parameters and under different boundary conditions. For this case in Eq. (6), by $k=0$, $E(z)$ convert to material elastic constant for isotropic conical shell [13] and we use it for our calculations. Before the results, let us introduce the following notation:

$$\rho_{cr}=\frac{P_{cr}}{P_{CL}} \quad (14)$$

where P_{cr} is the critical buckling loads obtained from the present method, and P_{CL} is the classical value of the critical buckling load

$$P_{CL}=\frac{2\pi Eh^2\cos^2\alpha}{\sqrt{3(1-\nu^2)}} \quad (15)$$

The above equation is suggested by Siede and Calif [1]. The present values P_{cr} and their comparison with those in Ref. [7] are shown for isotropic cones with different values of L/R_1, semi-vertex angles α and different boundary conditions, i.e. SS1 and SS3 in Table 1, SS2 in Table 2, SS4 in Table 3 and CC1 and CC3 in Table 4. Good agreement for ρ_{cr} can be observed between the present results and those from Baruch et al. [7]. There is, however, a difference in the circumferential wave number. It can be seen that ρ_{cr} tends to 0.5 for SS1, SS2 and SS3 and to 1.0 for SS4, CC1 and CC3. This means that there exists a lower critical value for SS1, SS2 and SS3. Siede's

formula is only applicable to SS4, CC1 and CC3. For extremely short cones with $L/R_1 = 0.2$, ρ_{cr} becomes larger as α increases and ρ_{cr} tends to a constant independent of α for cones with L/R_1 larger than 0.5.

Table 1
Critical loads ratio ρ_{cr} for SS_1 and SS_3 boundary conditions ($R_1/h = 100.0$, $\upsilon = 0.3$)

α	L/R_1=0.2	L/R_1=0.2	L/R_1=0.5	L/R_1=0.5
	Present	Baruch et al. [7]	Present	Baruch et al. [7]
1°	0.5032	0.4991	0.5131	0.5131
5°	0.5057	0.5021	0.5142	0.5139
10°	0.5106	0.5075	0.5151	0.5147
20°	0.5280	-	0.5163	-
30°	0.5616	0.5567	0.5140	0.5139
45°	0.6491	-	0.4947	-
60°	0.8715	0.8701	0.4486	0.4486
70°	1.2346	-	0.4304	-
80°	2.3832	2.3830	0.5405	0.5407

Table 2
Critical loads ratio ρ_{cr} for SS_2 boundary condition ($R_1/h = 100.0$, $\upsilon = 0.3$)

α	L/R_1=0.2	L/R_1=0.2	L/R_1=0.5	L/R_1=0.5
	Present	Baruch et al. [7]	Present	Baruch et al. [7]
1°	0.5081(1)	0.5106(2)	0.5147(1)	0.5191(2)
5°	0.5098(1)	0.5133(2)	0.5153(1)	0.5191(2)
10°	0.5102(1)	0.5184(2)	0.5163(1)	0.5203(2)
20°	0.5284(1)	-	0.5179(1)	-
30°	0.5604(1)	0.5696(2)	0.5166(1)	0.5203(2)
45°	0.6534(1)	-	0.4992(1)	-
60°	0.8759(1)	0.8924(2)	0.4596(1)	0.4652(2)
70°	1.2428(1)	-	0.4423(1)	-
80°	2.3997(1)	2.4470(2)	0.5572(1)	0.5984(2)

Table 3
Critical loads ratio ρ_{cr} for SS_4 boundary condition ($R_1/h = 100.0$, $\upsilon = 0.3$)

α	L/R_1=0.2	L/R_1=0.2	L/R_1=0.5	L/R_1=0.5
	Present	Baruch et al. [7]	Present	Baruch et al. [7]
1°	1.0051(7)	1.005(7)	1.0020(8)	1.002(8)
5°	1.0057(7)	1.006(7)	1.0018(8)	1.002(8)
10°	1.0071(7)	1.007(7)	1.0012(8)	1.002(8)
20°	1.0097(6)	-	1.0000(8)	-
30°	1.0171(5)	1.017(5)	1.0006(7)	1.001(7)
45°	1.0415(2)	-	1.0110(5)	-
60°	1.1443(0)	1.144(0)	1.0032(5)	1.044(7)
70°	1.4207(0)	-	1.0150(5)	-
80°	2.4774(0)	2.477(0)	1.0111(3)	1.015(5)

Table 4
Critical loads ratio ρ_{cr} by present method

α	L/R_1=0.2	L/R_1=0.5	L/R_1=0.2	L/R_1=0.5
	CC_1	CC_1	CC_3	CC_3
1°	1.664(0)	1.004(8)	-	1.053(8)
5°	1.678(0)	1.007(8)	1.678(0)	1.054(8)
10°	1.708(0)	1.006(8)	1.709(0)	1.064(8)
30°	1.945(0)	1.002(7)	1.947(0)	1.099(8)
45°	2.372(0)	0.999(5)	2.375(0)	1.029(0)
60°	3.320(0)	1.001(2)	3.328(0)	1.015(0)

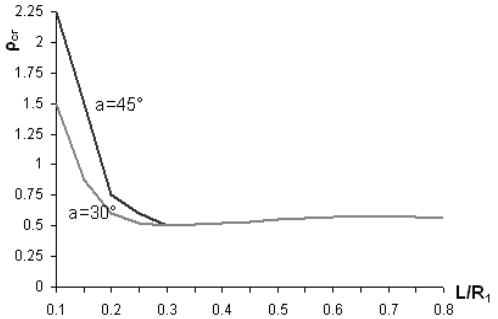

Fig. 2
Influence of L/R_1 on ratio ρ_{cr} for SS_3.

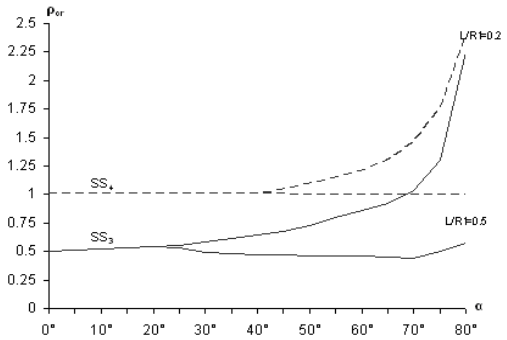

Fig. 3
Influence of α on ratio ρ_{cr} for SS_3 (R_1/h=100, υ=0.3).

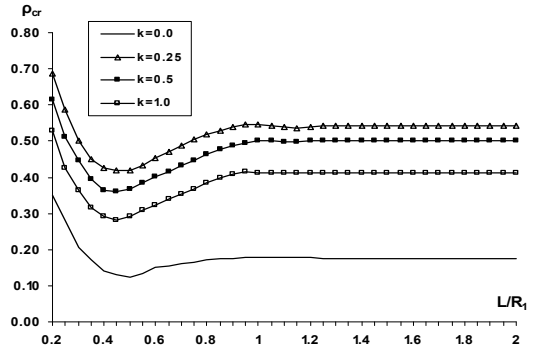

Fig. 4
Influence of L/R_1 on ratio ρ_{cr} for SS_3
($\alpha = 30^{\circ}$, $R_1/h = 100$, $\upsilon = 0.3$).

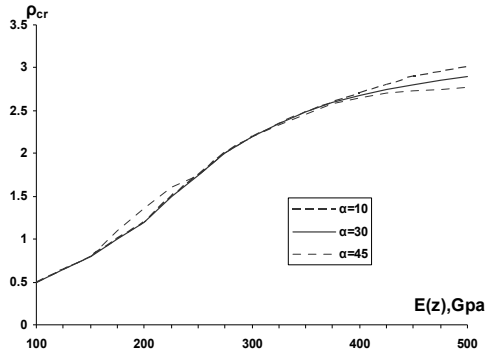

Fig. 5
Influence of $E(z)$ on ratio ρ_{cr} for SS_3 ($L/R_1=10,\ R_1/h=100,\ \upsilon=0.3$).

These properties are shown in Fig. 2 for SS3 and Fig. 3 for SS3 and SS4. Another important phenomenon worth noting is that the buckling wave number tends to decrease as α increase.

4.2. Numerical results for FGM cones

For FGM cones, we compute for ρ_{cr} from Eq. (15) with E replaced by $E(z)$. Numerical results for functionally graded cones with SS3 are shown in Fig. 4, from which the influence of L/R_1 on ρ_{cr} for cones with the combination of materials consists of aluminium and alumina with different values of k, may be noted. The Young's modulus for aluminium is, $E(m)=70$ Gpa and alumina is $E(c)=380$ Gpa. It can be seen that ρ_{cr} is independent of L/R_1 when L/R_1 is larger than 1.0, and also ρ_{cr} first decreases and then increases as L/R_1 increases from 0.2 to 1.0. This curves the same variation as it has been shown in Fig. 2. Fig. 5 shows the effect of $E(z)$ on ρ_{cr} for FGM cones with parameters given in the figure. It can be observed that ρ_{cr} increases as $E(z)$ becomes large and it approaches a constant when $E(z)$ is large enough. It is also noteworthy that semi-vertex angle α has a slight effect on ρ_{cr}, and there exists only a slight difference among ρ_{cr} for $\alpha=10^\circ, 30^\circ$ and 45°.

5 CONCLUSION

The salient points in this study include: (1) Derivation of a systematic solution procedure for buckling analysis of isotropic conical shells under axial compression and external pressure, using the power series method; (2) The application of the solution to all types of boundary conditions and to various kinds of truncated conical shells; (3) The identification of effects of semi-vertex angle and material constants on the buckling loads.

REFERENCES

[1] Siede, P., Calif, L.A., 1956, Axisymetric buckling of circular cones under axial compression, *ASME Transactions*, *Journal of Applied Mechanics* **23**: 625-628.
[2] Lackman L., Renzien J., 1960, Buckling of circular cones under axial comperession, *ASME Transactions*, *Journal of Applied Mechanics* **27**: 458-460.
[3] Singer J., 1961, Buckling of circular conical shells under axisymmetrical external pressure, *Journal of Mechanical Engineering Science* **3**: 330-339.
[4] Singer J., 1965, Buckling of circular conical shells under uniform axial compression, *AIAA Journal* **3**: 985-987.
[5] Weigarten V.I., Seide P., 1965, Elastic stability of thin walled cylindrical and conical shells under combined external pressure and axial compression, *AIAA Journal* **3**: 913-920.
[6] Weigarten V.I., Seide P., 1965, Elastic stability of thin walled cylindrical and conical shells under combined external pressure and axial compression, *AIAA Journal* **3**: 1118-1125.

[7] Baruch M., Harari O., Singer J., 1970, Low buckling loads of axially compressed conical shells, *ASME Transactions*, *Journal of Applied Mechanics* **37**: 384-392.
[8] Tani J., Yamaki Y., 1970, Buckling of truncated conical shells under axial compression, *AIAA Journal* **8**: 568-570.
[9] Singer J., 1966, Buckling of damped conical shells under external pressure, *AIAA Journal* **4**, 328-337.
[10] Baruch M., Singer J., 1965, General instability of stiffened conical shells under hydrostatic pressure, *Aeronautics Quarterly* **26**: 187-204.
[11] Weigarten V.I., Morgan E.J., Seide P., 1965, Elastic stability of thin walled cylindrical and conical shells under axial compression, *AIAA Journal* **3**: 500-505.
[12] Tong Liyong, 1988, Buckling and vibration of conical shells composed of composite materials, Ph.D. Thesis, Beijing University of Aeronautics and astronautics.
[13] Reddy J. N., Praveen G. N., 1998, Nonlinear transient thermoelastic analysis of functionally graded ceramic-metal plates, *International Journal of Solids and Structures* **35:** 4467-4476.
[14] Tong L., Tabarrok B., Wang T.K., 1992, Simple solution for buckling of orthotropic conical shells, *International Journal of Solids and Structures* **29:** 933-946.